

Progressive collapse resistance of flat slabs: modeling post-punching behavior

Yaser Mirzaei^a and Mehrdad Sasani*

Northeastern University, 400 Snell Engineering Center, Boston, MA 02115, USA

(Received April 5, 2012, Revised March 18, 2013, Accepted August 29, 2013)

Abstract. Post-punching resistance of a flat slab can help redistribute the gravity loads and resist progressive collapse of a structure following initial damage. One important difficulty with accounting for the post-punching strength of a slab is the discontinuity that develops following punching shear. A numerical simulation technique is proposed here to model and evaluate post-punching resistance of flat slabs. It is demonstrated that the simulation results of punching shear and post-punching response of the model of a slab on a single column are in good agreement with corresponding experimental data. It is also shown that progressive collapse due to a column removal (explosion) can lead to punching failure over an adjacent column. Such failure can propagate throughout the structure leading to the progressive collapse of the structure. Through post-punching modeling of the slab and accounting for the associated discontinuity, it is also demonstrated that the presence of an adequate amount of integrity reinforcement can provide an alternative load path and help resist progressive collapse.

Keywords: progressive collapse; punching shear; post-punching; flat slab; finite element method; failure

1. Introduction

After terrorist attacks on the Murrah Federal building in 1995 and on the World Trade Center towers and the Pentagon on September 11, 2001, a new wave of research started to experimentally as well as analytically evaluate progressive collapse resistance of structures (Sozen *et al.* 1998, Corley 2004, Sasani *et al.* 2007, Bao *et al.* 2008, Sasani and Sagioglu 2008). Progressive collapse is defined as the spread of an initial local failure from element to element, which eventually results in the collapse of an entire structure or a disproportionately large part of it (ASCE-7 2010). Following the occurrence of initial damage to a structural system due to an explosion, vehicle impact, or other man-made or natural hazards, progressive collapse resistance is typically accomplished by providing alternative load paths to redistribute gravity loads. Progressive collapse is arrested if collapse does not progress beyond certain specified limits. The actual cause of initial damage to the gravity load-bearing system is usually not specified in the design or evaluation procedure (a threat independent approach) and the damage is assumed to be sudden and permanent.

*Corresponding author, Associate Professor, E-mail: sasani@neu.edu

^aStructural Engineer, E-mail: yaser.mirzaei@wspgroup.com

The alternative path method for progressive collapse analysis of structures is used in the design guidelines issued by the General Services Administration (GSA 2003) and the Department of Defense (DOD 2010). These guidelines are meant to evaluate general integrity of structures and their capacity to redistribute the loads following initial damage. The analysis method typically assumes that a single column of a building is suddenly removed and the capacity of the remaining structural system to bridge over the damaged area is evaluated. After column removal, the loads previously carried by the column will be dynamically redistributed to the neighboring elements, which could lead to partial or entire collapse of the structure.

In flat plate systems, one potential source of progressive collapse in neighboring columns is punching shear caused by the transfer of additional loads from the removed columns. Punching failure of flat slabs without shear reinforcement is brittle and occurs with almost no warning. Over the past decades, several collapses due to punching shear failure occurred that resulted in human casualties and large damages (Schousboe 1976, Carino *et al.* 1983, Kaminetzky 1991, King and Delatte 2004, Ellingwood *et al.* 2007). These collapses have clearly demonstrated the possible disastrous consequences of punching shear failure.

Following loss of a column and the subsequent dynamic load redistribution, punching failure can occur and propagate through the slab and eventually lead to the collapse of entire or a large part of the structure. Studying post-punching behavior of flat slabs can help adopt mitigating strategies to enhance structural robustness and to reduce the likelihood of the progressive collapse. In this paper, first a modeling technique is proposed to evaluate punching and post-punching response at a local level, i.e., slab on a single column. The simulation results obtained from this model are compared with experimental data (Mirzaei and Muttoni 2008, Mirzaei 2010). Then to evaluate the effects of punching shear in progressive collapse analysis of structural systems, the response of a flat slab structure following loss (explosion) of a column leading to punching shear failure in a neighboring column is studied.

2. Punching shear failure in reinforced concrete slabs

The design of reinforced concrete (RC) flat slabs is primarily governed by deflection at the serviceability limit state and punching shear at the ultimate limit state. If a slab is overloaded, for instance due to an accident, seismic ground motion, or an explosion, punching shear failure can occur. When no punching shear reinforcement is provided, punching failure occurs in a brittle manner with almost no warning signs. The response of an RC slab under a monotonic increasing load (displacement) starts with a linear elastic behavior. Flexural cracks will appear next and the slab longitudinal reinforcement may or may not yield prior to the punching shear failure (Muttoni 2008). Following the punching failure, the capacity of the slab to transfer loads to the column drops drastically with an increase of the vertical displacement until a minimum load resistance is reached. Beyond this stage, the behavior of the slab will depend on redundancy, continuity, integrity, deformation capacity, and reinforcement layout (Hewitt and Batchelor 1975, Mitchell and Cook 1984). And finally, the total failure occurs when the axial strains of the reinforcing bars reach the ultimate tensile strain of the reinforcement (Park 1964).

2.1 Cracking

Prior to punching, radial and tangential flexural cracks are usually formed on the tension (top)

side of the slab in the vicinity of the column. A roughly circular tangential crack forms near the projection of the column perimeter and radial cracks extend from that area (ACI-ASCE Committee 426 1974). The distribution of the radial moment is roughly constant in the vicinity of the column but it decreases rapidly with distance from the column.

The punching shear failure occurs when a critical shear crack (usually initiated from a flexure crack) forms, propagates through the slab and starts to open. The development of the critical shear crack does not necessarily imply the immediate collapse of the member. As the shear crack reaches the compression zone of the slab, some new shear-carrying mechanisms such as arching action and aggregate interlocking are developed (Muttoni 2008). These shear-carrying mechanisms are active at punching failure.

Generally, it is intricate to track down the development of the critical shear crack in concrete slabs. However, Guandalini (2005) could measure the opening of the critical shear. Based on experimental studies, the shear crack initiates around 50-70% of the punching load, and the crack width opens up to 1.0 to 1.5 mm before punching failure occurs (Theodorakopoulou and Swamy 2002, Guandalini 2005). The formation of the critical shear crack can alter the shear transfer mechanism right before punching failure. It has been observed that the radial compressive strain at the bottom of the slab and in the vicinity of the column starts to decrease at about 80% of the ultimate load and even tensile strain was observed shortly before punching (Muttoni 2008). This phenomenon can be expressed as a stage of redistribution of internal forces, which is necessary to maintain force equilibrium in the radial direction (Muttoni 2008, Muttoni and Fernández 2008). At this stage, reinforcing bars passing through the punching cone are activated and contribute to the shear transfer mechanism.

2.2 Shear strength as a function of deformation capacity

Muttoni has recently developed a failure criterion for slabs which determines the slab punching strength primarily as a function of the radial rotation of the slab in the vicinity of the slab-column connection (Muttoni 2008, Muttoni and Fernández 2008, Guandalini *et al.* 2009). Based on their research, the development of the critical shear crack reduces the shear strength significantly. They experimentally showed that the radial compressive strain in the soffit of the slab in the vicinity of the column begins to decrease after reaching a maximum shortly before punching. In fact, the critical shear crack which passes through the inclined compression strut carrying the shear force to the column reduces the radial compressive strength and thus reduces the shear strength. The relationship between the opening of the critical shear crack (slab rotation near the column) and the punching shear strength provide a fundamental theory for the proposed failure criterion. To compute the punching strength, the load-rotation relationship of the slab is needed for which a quadrilinear moment-curvature relationship for the RC section was developed (Muttoni 2008). The failure criterion accounts for various shear transfer mechanisms including aggregate interlocking but not explicitly dowel action.

2.3 Contribution of longitudinal reinforcement

The contribution of longitudinal reinforcement to punching load has been known for a long time (Kinnunen and Nylander 1960, Long 1975, Hewitt and Batchelor 1975) but did not appear in codes of practice and design guidelines because the phenomenon is complex and this contribution is rather difficult to quantify. The first rational model of punching shear was proposed by

Kinnunen and Nylander (1960) more than 50 years ago. The model, however, did not explicitly estimate the contribution of the longitudinal reinforcement to the shear transfer and therefore a correction factor of 1.1 was incorporated to account for this contribution (Fib 2001). It was stated that the mechanism of shear transfer through the longitudinal reinforcement was dowel action and its contribution was only about 10% of the punching shear strength. Hewitt and Batchelor (1975), however, concluded that the contribution of dowel action was more significant and that the punching strength could be enhanced by 20% due to dowel forces. Long (1975) went even further and stated that the dowel forces contributed approximately 30% of the punching strength. Despite large scientific efforts devoted to dowel action investigation, there is still no unanimity on this shear transfer mechanism and on the reliability of this action (Jelic *et al.* 1999). In general, dowel action becomes active as soon as the punching shear crack reaches the compression zone of the slab and crosses the slab bottom reinforcement. Note that the slab bottom reinforcement crossing over the column is called the integrity reinforcement, which is under compressive stress before punching shear. For small displacements after punching, dowel action undoubtedly contributes to the shear transfer, but vanishes quickly as the relative vertical displacement between the slab and punching cone increases. For larger displacements after punching, reinforcing bars act in a hammock-like fashion suspending the slab and keeping it from falling down (Knoll and Vogel 2009).

Kinnunen and Nylander (1960) tested a series of slabs investigating the influence of the reinforcement ratio on the punching response. They observed a ductile behavior with yielding of the entire tensile rebars for slabs with low reinforcement ratios ($\rho = 0.5\%$), but they recorded a very brittle behavior without reinforcement yielding for slabs with large reinforcement ratio ($\rho = 1.5\%$). For moderate reinforcement ratio, a brittle behavior was observed accompanied by some reinforcement yielding.

In a slab with a small flexural reinforcement ratio, the yielding of the rebars limits the slab flexural strength and in turn the ultimate load the slab can carry. As a result, the maximum load that the slab can transfer to the column is small. On the other hand, a slab with a larger flexural reinforcement ratio can carry and transfer a larger load to the column. Therefore, if both slabs fail in punching shear, the slab with smaller flexural reinforcement will experience a smaller shear demand limited by the slab flexural strength. That is, while the slab with a smaller amount of flexural reinforcement will punch under a smaller shear force, this occurs due to excessive rotation from flexural yielding. The shear force at which punching occurs is in fact the shear demand, which is limited by a smaller flexural strength.

2.4 Post-punching shear transfer

Three failure zones can be characterized as shown in Fig. 1. For zone 1, the reinforcing bars act against the concrete cover. The spalling of the concrete cover is the governing mode of failure. For further deflection, reinforcing bars tend to tear out of concrete and become detached from the concrete surface (Melo and Regan 1998). For zone 2, the thickness of the concrete at the location where the reinforcing bars cross the punching cone is small and as a consequence concrete breakout occurs (Mirzaei 2010). For zone 3, which is similar to zone 2, the same scenario occurs. The only difference refers to the concrete supporting the bar. Zone 3 is on the compression side of the slab and the concrete is barely cracked. However, zone 2 is on the tension side of the slab where the concrete is severely cracked due to bending and shear.

For the specimens including integrity reinforcement Mirzaei and Muttoni reported that the

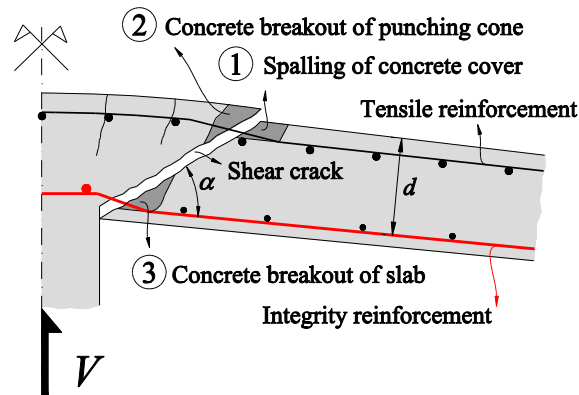


Fig. 1 Failure zones after punching shear failure

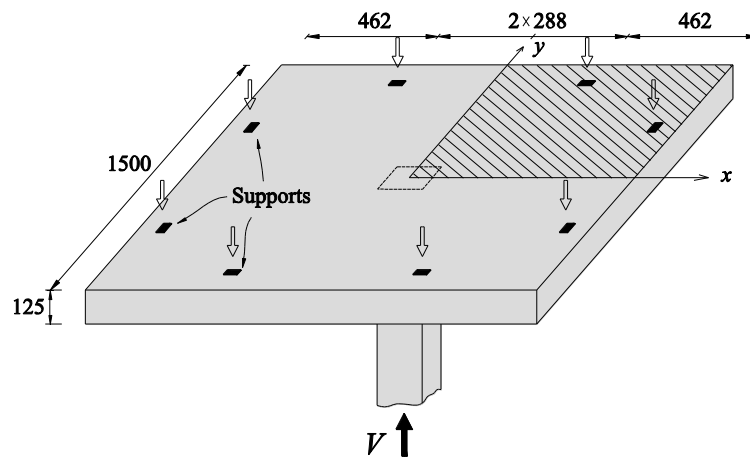


Fig. 2 Typical half-scale slab specimen (All dimensions in mm)

failure process in zones 2 and 3 started by the concrete breakout up to a certain point and then stopped (Mirzaei and Muttoni 2008). Beyond this point, the thickness of the concrete was enough to prevent the concrete from breaking out. If the concrete thickness is larger than six to eight times the bar diameter, concrete breakout does not occur and the failure resulted from fracture of the bar ($f_u < 700$ MPa). In general, the contribution of the integrity reinforcement to the post-punching strength is governed either by the maximum breakout strength of the concrete above the bar or by the fracture of the integrity bars.

3. Numerical simulation of slab on a single column

In most experimental work on the punching shear, a slab specimen represents an area over the column subjected to negative radial moment (tension at the top). The edges of the slab represent the lines of zero radial moments and hence the length of the specimen is limited by the points of inflection of the slab. The distance between the column axis and the perimeter where the radial bending moments are zero is approximately $0.22 L$ (linear elastic behavior and Poisson ratio = 0.15)

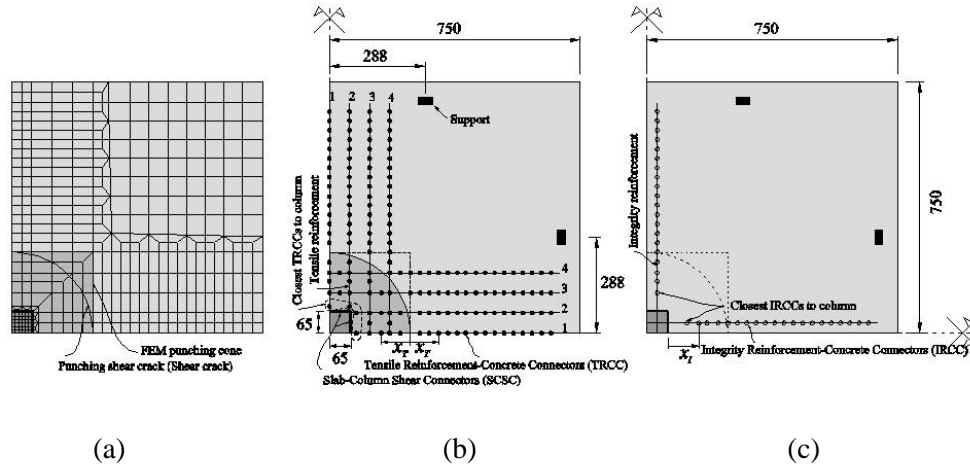


Fig. 3 Modeling slab on a single column: (a) FEM mesh; (b) tensile reinforcement and its connectors (TRCC); and (c) integrity reinforcement and its connectors (IRCC)

and therefore the dimension of the slab specimen is $0.44 L$. For instance, a half-scale slab specimen with a 1.5 m length represents a floor slab with a span of $L = 7$ m. As a part of an extensive experimental program on the post-punching behavior of flat slabs (Mirzaei and Muttoni 2008), Mirzaei tested a half-scale simply supported slab specimen (PM-11) shown in Fig. 2 under a monotonically increasing displacement at the location of the column. The slab thickness was 125 mm. Fig. 3(a) shows a Finite Element Model (FEM) of the slab. Only one quarter of the slab (hatched area in Fig. 2) is modeled due to symmetry. In this paper the computations are performed using the *explicit time integration version* of the commercially available finite element software ABAQUS version 6.9.

3.1 Materials

Using experimental data, the tensile (f_{ct}) and compressive (f'_c) strengths of the concrete are set at 2.5 MPa and 32.3 MPa, respectively. The modulus of elasticity of the concrete is 33 GPa and its Poisson's ratio is 0.15. The reinforcing steel is modeled as a quadrilinear elastic-plastic material with strain hardening. The modulus of elasticity of steel reinforcement is 200 GPa, the yield strength is 548 MPa, and the ultimate tensile strength is 625 MPa. The ultimate strain is 0.074 for the tensile reinforcement and 0.105 for the integrity reinforcement.

3.2 Shell elements

The four-node first-order quadrilateral shell S4R with reduced integration points and finite strains from the Abaqus element library (Abaqus INC 2010) is used to model the slab. As described before, in slabs with a high longitudinal reinforcement ratio (as is the case for the slab studied in this paper), punching can occur before flexural yielding (Kinnunen and Nylander 1960). Furthermore, the focus of this study is on modeling the punching and post-punching response of the slab. Therefore, the model nonlinearity is implemented only at the location of punching shear

and the slab away from this area is modeled linearly. To account for the effects of the concrete cracking, the flexural stiffness of the slab is reduced to one-quarter of the gross section flexural stiffness, $0.25E_cI_g$ (ACI 318 2011).

3.3 Slab-Column Shear Connectors (SCSC)

Two different phases that can be distinguished in the load-deflection response of a slab where punching failure occurs are the pre- and post-punching phases. The post-punching behavior is simulated explicitly in this paper. The slab punching strength is estimated at 241 kN using the Critical Shear Crack Theory (Muttoni 2008, Muttoni and Fernández 2008). In the model developed in this paper the effects of dowel action on punching shear strength is explicitly accounted for. Based on the discussion presented in the Contribution of longitudinal reinforcement Section, it is assumed that 15% of the punching strength is provided by dowel action (Kinnunen and Nylander 1960, Hewitt and Batchelor 1975, Long 1975, Muttoni and Fernández 2008). Therefore, the contribution of the concrete slab in punching strength is assumed to be 85% of the estimated punching strength ($V_{conc} = 0.85V_p$). This assumption will be evaluated and discussed later.

In order to model punching shear, the slab is connected to the column using Slab-Column Shear Connectors (SCSC). From the available connector elements in Abaqus, the Cartesian + Cardan connector has been selected in this study. All six components of relative motions (degrees of freedom, dof) are available for this connector. In other words, this connector can relate all six dof of the two nodes it connects together. If a failure criterion defined for one of the connecting dof is met, the program allows either all the connected dof or only the single dof fail. In punching shear failure, the former occurs upon reaching the punching strength of the slab. That is, while before punching a SCSC connects a slab node to the adjacent node in the perimeter of the column section, after the shear force in the connector reaches its shear strength ($F_{c,max}$) failure value, all six connected dof fail simultaneously. Or in the case of a column under pure axial force, when the compressive force in the column exceeds the punching strength of the slab, the entire connection fails. In order to find the shear strength of each connector, the shear strength provided by the concrete slab discussed in the previous paragraph is divided by the number of connectors ($N_c = 52$) used around the column full section, which is the same as the number of nodes around the column section.

These connectors are implemented to simulate the shear transfer from the slab to the column while maintaining the continuity of other internal forces before punching shear occurs. The shear behavior of the connectors will be defined accordingly while a rigid behavior is chosen for the

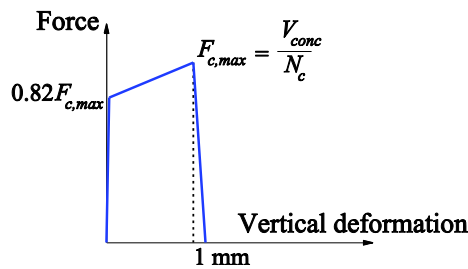


Fig. 4 Constitutive law of Slab-Column Shear Connectors (SCSC)

other five components of relative motions. Fig. 4 shows the constitutive law (force versus vertical deformation) for the shear behavior of the connectors. The behavior is set to be practically rigid up to 82% of the connector vertical shear strength ($0.82F_{c,max}$). As discussed before, 85% of the shear strength is assumed to be provided by the concrete (and the rest by dowel action). Therefore the shear stiffness of the connectors will be reduced when the column force reaches about 70% of punching strength ($0.82 \times 0.85V_p = 0.70V_p$), which is the upper limit for shear cracks to develop (Theodorakopoulou and Swamy 2002, Guandalini 2005). When the shear crack starts to open, the shear connectors become more flexible. At this point, the longitudinal reinforcement starts to contribute to the shear transfer, modeling dowel action. As mentioned before, the critical shear crack opens up to about 1.0 to 1.5 mm in the vertical direction before punching (Guandalini 2005). To account for the opening of the shear crack, a 1 mm vertical deformation at punching is assigned to the shear connectors as shown in Fig. 4. Eventually, when the force in the connectors reaches $F_{c,max}$, the connectors break free and the punching shear failure occurs.

3.4 Punching cone

After punching shear failure, the critical shear crack will introduce a discontinuity surface to the slab. A punching cone will form at the top of the column and the slab will be attached to the cone only through the longitudinal reinforcement. As shown in Fig. 1, the tensile and integrity reinforcement cross the critical shear crack at different distances from the column. The tensile reinforcement crosses the punching cone at the distance of $d \cdot \cot \alpha$ from the face of the column (Zones 1 and 3) where d is the effective depth of the concrete slab and α is the angle of inclination of the punching cone with respect to a horizontal plane (see Fig. 1). The integrity reinforcement crosses the punching cone approximately at the face of the column.

In order to account for the discontinuity after punching shear failure, the punching cone is modeled explicitly. That is, in addition to the slab that is connected to the column through the SCSC, a punching cone is attached to the top of the column. There is no vertical gap between the slab and the punching cone before punching. After punching, however, the slab will move downwards with respect to the column and the punching cone, see Fig. 5. For clarity, the tensile reinforcing bar is shown in the right half and the integrity reinforcement is shown in the left side of Fig. 5. As can be seen, the punching cone and the slab are connected only through the tensile reinforcement. Note that the integrity reinforcement connects the slab directly to the column. To facilitate the mesh generation, a square punching cone has been used instead of the circular one as can be seen in Fig. 3. This simplifies the meshing and allows generating nodes in the punching cone which are aligned with the slab nodes and facilitate connecting tensile reinforcing bars to both the slab and the punching cone. The geometry of the shell elements in the punching cone is

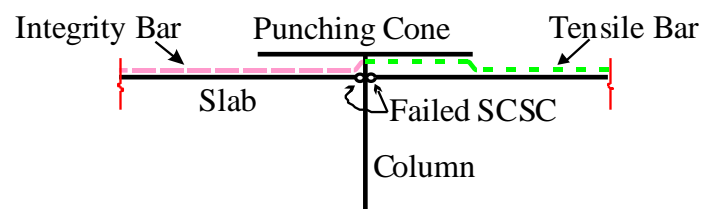


Fig. 5 Schematic representation of slab and punching cone soon after punching failure. While model is symmetric, on left side only integrity bar and on right side only tensile bar is shown

the same as that in the slab. The reinforcing bars are connected only the part of the square cone that is within the actual circular punching shear crack, which will be discussed in the following sections.

The thickness of the punching cone is not constant and varies from zero where the shear crack reaches the tension surface of the slab to the thickness of the slab at the column face. This fact should be accounted for in the finite element modeling and thus the shell elements of the punching cone have variable thickness. The refined simulation of this variation is computationally expensive and hence the variation of the concrete thickness is simulated by using different concrete thicknesses for the shell elements. The shell elements of the punching cone close to the column are thicker while those far from the column are thinner. The gradual variation has been achieved in six steps. The thickness of each shell element is set equal to that of the actual punching cone at the center of the element.

3.5 Reinforcing bars

The two-node first-order Bernoulli beam element B31 (Abaqus INC 2010) has been chosen to simulate the reinforcing bars, shown in Figs. 3(b) and (C). Reinforcing bars will be activated representing dowel action soon after the shear crack starts to open, i.e., when the SCSCs start to become flexible. The vertical component of the axial tensile force developed in each reinforcing bar is its contribution to the post-punching shear transfer.

3.6 Reinforcement-Concrete Connectors (RCC)

Connectors representing the interaction between tensile reinforcement and concrete within the punching cone (concrete breakout) in Zone 2 (Fig. 1) are generated between two adjacent nodes one from the punching cone and another from the tensile reinforcement. Similarly, connectors representing the interaction between tensile reinforcement and concrete slab outside of the punching cone (spalling of concrete cover) in Zone 1 connect nodes in the slab to the adjacent nodes of the tensile reinforcement. The connectors connecting the integrity reinforcement to the slab are generated between two nodes one from the slab and another from the integrity reinforcement.

As pointed out earlier, various types of failure take place when a column punches through the slab. Concrete breakouts occur, which are associated with the integrity reinforcement (zone 3 in Fig. 1) and the tensile reinforcement (zone 2 in Fig. 1). Also, spalling of the slab concrete cover associated with the tensile reinforcement occurs outside of the punching cone (zone 1 in Fig. 1). The mechanism of these failures are rather complex but their ultimate strength (concrete breakout and spalling strengths) can be reasonably estimated. For instance, according to ACI 349 (2001), the breakout strength can be calculated as the sum of the vertical components of forces developed by the tensile stresses acting on the surface of a concrete breakout. In order to model concrete breakout and spalling, the reinforcing bars are connected to the concrete using Reinforcement-Concrete Connectors (RCC). When the vertical force in an RCC exceeds the concrete strength, the breakout or spalling occurs.

Integrity Reinforcement-Concrete Connectors (IRCC)

The concrete breakout strength associated with the thickness of concrete above the integrity reinforcement as a function of the distance from the face of the column, x_l , (see Fig. 3(c)) is

$$V_{break}(x_l) = A_{c,eff}(x_l)(\eta_l f_{ct}) \quad (1)$$

$$A_{c,eff}(x_l) = (x_l \tan \alpha)^2 \left[\theta_{x_l} + \frac{n}{2}(\pi - 2\theta_{x_l}) + \frac{n-1}{2} \sin 2\theta_{x_l} \right]$$

where V_{break} is the concrete breakout strength of all the IRCC on one side of the column and at distance x_l from the column face (see Fig. 3(c)). This strength can be approximately divided by the number of bars to find the strength of one IRCC. $A_{c,eff}$ is the horizontal projection area of the conical failure surface activated by the integrity reinforcement, f_{ct} is the tensile strength of concrete, n is the number of integrity bars passing through the column in one direction, s is the integrity bar spacing, $\cos \theta_{x_l} = s / (2x_l \tan \alpha)$, and α is defined before (see Fig. 1) and set equal to $\pi/6$ with respect to the horizontal plane. The reduction factor η_l is adopted to consider the variation of the tensile stress from a maximum at the edge of integrity reinforcing bars to a minimum at the crack surface ($\eta_l = 0.6$) (Mirzaei 2010). Each integrity reinforcing bar is connected to the slab nodes along the bar and their vertical strengths are calculated using Eq. (1). All degrees of freedom are constrained for IRCC except the component of motion which is associated with the vertical behavior of the connector. The IRCC in the vertical direction behaves practically rigid up to failure.

Tensile Reinforcement-Concrete Connectors (TRCC)

The same approach can be adopted for using nonlinear connectors to simulate the concrete breakout within the punching cone and spalling of the concrete cover outside of the punching cone for the tensile reinforcement. The connectors simulating the concrete breakout strength connect the tensile reinforcement to the punching cone. The connectors simulating the spalling strength of the concrete cover connect the tensile reinforcement to the slab. The spalling strength (V_{spall}) and the concrete breakout strength (V_{break}) associated with the tensile reinforcement can be calculated by

$$V_{spall}(x_T) = \pi c(D + 2x_T)(\eta_T f_{ct}) \quad (2)$$

$$V_{break}(x_T) = \pi x_T \tan \alpha (D - 2x_T)(\eta_T f_{ct})$$

where x_T is the radial distances from the punching crack (see Fig. 3(b)). $D = a + 2d \cot \alpha$ is the diameter of the original punching cone where a is the column width, d is the effective depth of the slab,

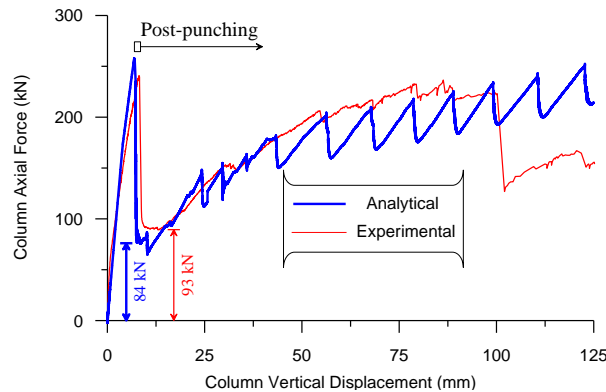


Fig. 6 Column axial force versus column top vertical displacement

and c is the concrete cover. Similar to η_I used in Eq. (1), a reduction factor $\eta_T = 0.4$ is used in Eq. (2) (Mirzaei 2010). The spalling and breakout strength for each TRCC is found by dividing V_{spall} and V_{break} by the number of bars at the same distance from the punching shear crack. The number of bars can be found by drawing an imaginary circle at a distance x_T from the punching shear crack (see Fig. 3(b)) and count the reinforcing bars that cross this circle.

3.7 Location of first connectors

For large displacements, it has been shown that the location of the first connector does not influence the post-punching strength, but the post-punching resistance right after punching is drastically affected by this distance (Mirzaei 2010). A part of the concrete slab breaks right after punching due to excessive shear and bending. The length of the broken concrete along the bar is practically unknown but a value of eight times the bar diameter can be chosen which gives a good agreement with the available experimental data. Given the shell element sizes and in turn the locations of the nodes, the first IRCC is located at a distance of 90 mm ($\approx 8 \times 12$ mm for integrity bar diameter of 12 mm) from the face of the column and the distance between the first TRCC on each side of the shear crack is about 60 mm ($\approx 8 \times 8$ mm for tensile bar diameter of 8 mm).

4. Simulation results and comparison with experimental data

Results obtained from the nonlinear finite element analysis (FEA) are compared with the experimental data in this section. Fig. 6 compares the column force versus the column top vertical displacement of the specimen PM-11 (Fig. 2) with the calculated response from by the nonlinear FEA. A good agreement can be found between the measured and calculated punching and post-punching response. The calculated result overestimates the punching strength. The punching strength of slab PM-11 from the experiment was 241 kN while the FEA found a punching strength of 262 kN (8.7% larger). As discussed before, the contribution of the reinforcement is assumed to be 15% of the punching strength. The simulation results show that the contribution of the reinforcement in shear transfer at punching is larger and about 24% of the punching strength. The total shear strength provided by dowel action is calculated at 64 kN (34 kN from the tensile reinforcement and 30 kN from the integrity reinforcement). Two different phases can be identified for the reinforcement contribution to the shear transfer regarding opening of the critical shear crack. This contribution is negligible up to a certain load level (assumed to be about 70% of punching strength in this paper) because the crack opening has not occurred yet. The shear crack starts to open as this load level is reached and as a consequence the shear stiffness of the slab-column connection drops, which is modeled by making the slab-column shear connectors more flexible. During this phase, a portion of the load is transferred by dowel action and the rest by the SCSCs. The SCSCs fail as punching shear occurs and the entire load is then transferred by the reinforcement.

The FEA slightly underestimates the column axial force right after punching failure (see Fig. 6). A value of 84 kN is obtained analytically, while a minimum shear strength of 93 kN was recorded during the experiment (PM-11). The sudden drops in the analytical response are associated with the failure of discretized IRCCs. Whenever an IRCC fails, the unsupported length of the bar increases and its angle of inclination decreases resulting in a sudden decrease of the vertical force transferred by the bar. These drops were not observed in the experiment due to the

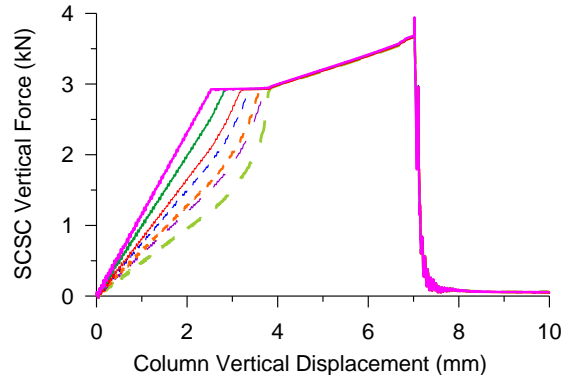


Fig. 7 Shear forces in Slab-Column Shear Connectors (SCSC)

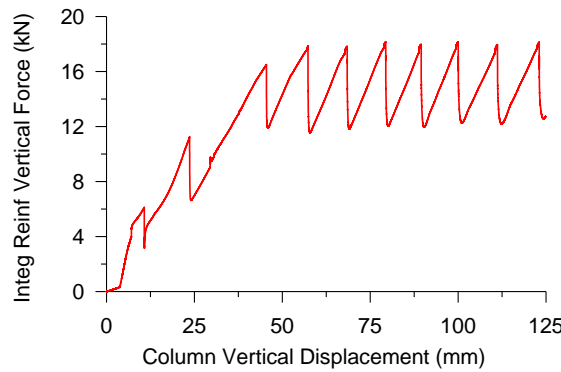


Fig. 8 Shear transferred through integrity reinforcement

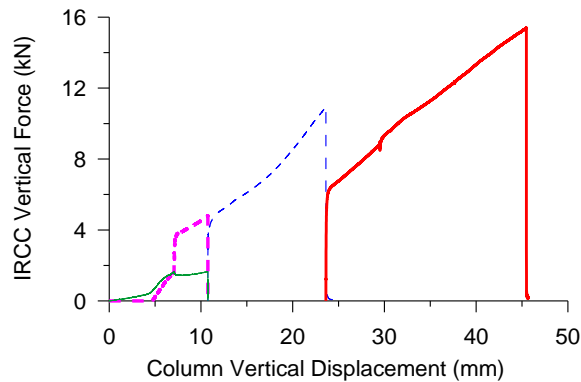


Fig. 9 Vertical forces of Integrity Reinforcement-Concrete Connectors (IRCC). Starting from closest IRCC to column, first four connectors fail (see Fig. 3b).

continuous nature of the process. As can be seen in Fig. 6, the experimental response drops significantly at about 100 mm vertical displacement. Two integrity bars fractured at this point during the test which was due to the excessive axial steel strain and local effects such as curvature localization (Mirzaei 2010). The simulation result does not capture this drop.

Fig. 7 shows the shear force versus column top displacement for seven SCSCs on one edge of

the column in the quarter-model of the slab (Fig. 3). As mentioned before, the SCSCs are included in the model to account for punching and therefore their strengths drop to zero after punching. As the column top displacement increases, although the same constitutive law is used for all SCSCs, the shear forces transferred to the connectors around the column are somewhat different due to the shape of column cross section. This difference is up to a certain point at which the connectors become more flexible and beyond this point their response is practically the same until the maximum strength has obtained. In other words, when the first connector becomes more flexible, the practically rigid neighboring connectors will carry most of the additional load. This shear force redistribution continues until all the connectors become flexible and start to deform together.

The contribution of one integrity reinforcing bar on one side of the column to the shear transfer is shown in Fig. 8. This contribution is negligible up to 3.8 mm column top displacement (associated with 70% of the punching strength and opening of the critical shear crack), but starts to increase after the critical shear crack widens. There is a jump in the shear transferred by the integrity reinforcement when the punching occurs (at the vertical displacement of 7.4 mm). This is attributed to a large relative displacement between the slab and the column after punching. As can be seen in the Figures, there are sudden drops in the response which is attributed to the breaking of the IRCCs. The vertical forces of the first four IRCCs and their breaking process are shown in Fig. 9.

The strength of the IRCCs depends on the thickness of the concrete over the integrity reinforcement, as described in Eq. (1). The thickness of the concrete associated with the first connectors is small and therefore the connector strength is small. For farther connectors from the shear crack, the thickness of the concrete increases and therefore stronger connectors are used. For the connectors away from the punching cone the thickness of the concrete is the same and equals to the slab effective depth. It should be mentioned that concrete breakout occurred vastly in the slabs tested by Mirzaei (2010) because the slabs were thin (125 mm thick) while in the real circumstances concrete breakout strength is not generally the governing failure mode.

The contribution of the tensile reinforcement to the shear transfer is shown in Fig. 10. Note that the contribution of reinforcing bars number 1 and 2 are practically identical. As for integrity reinforcement, this contribution is not pronounced up to the 70% of the punching strength (3.8 mm column deflection) but starts to increase after the critical shear crack opens. This behavior is followed by a jump in the tensile reinforcement contribution to the shear transfer when the punching occurs (at column displacement of 7.4 mm). The jump is followed by a drop in the response which is associated with the connector breaking. The simulation has shown that three weak TRCCs break right after punching resulting in the sudden decrease of the response (Fig. 11(a)). The TRCCs vertical force versus column displacement is shown in Fig. 11. With reference to Fig. 10, the significant difference between the contributions of different reinforcing bars to shear transfer is attributed to the geometry and slab boundary conditions. Some tensile reinforcement passes through the column and some of them do not and merely pass through the punching cone. The ones that pass through the column contribute to the shear transfer until the end of simulation unless their axial strain reaches the ultimate tensile strain. The ones that only cross the punching cone are active until their TRCCs reach their ultimate strength and break leaving these reinforcing bars ineffective.

Fig. 12 shows the deformed shape of an integrity reinforcement bar for column vertical displacements before and after punching. Note that punching occurs at a vertical displacement of 7.4 mm. The left hand side of the reinforcing bar is connected to the column and therefore moves with the column as the displacement increases (displacement controlled). The rest of the

reinforcing bar is connected to the slab and deforms with the slab. The two deformed shapes shown by dashed lines are before punching. After punching occurs and the slab drops with respect to the column, the part of the integrity reinforcing bar that is connected to the slab suddenly moves downwards and consequently the deformed shape of the reinforcing bar changes significantly. The slab deflection contours before and after punching failure are shown in Fig. 13. The significant difference between the graphs indicates the occurrence of the punching failure as the column penetrates into the slab. The slab deformation is less after punching because there is no continuity between slab and the punching cone and the only link is the longitudinal reinforcement.

The numerical simulation and the results for the post-punching response of flat slabs presented in this paper rely on the strength of both types of reinforcement-concrete connectors (RCC), i.e., the IRCC and TRCC. As mentioned before, the connectors represent the interaction between integrity and tensile reinforcing bars and concrete, and in turn the breakout and spalling strengths of concrete (see Fig. 1). The methods for calculating the concrete breakout and spalling strengths, and in turn the strength of the RCCs, are presented in detail in Mirzaei (2010). In his dissertation, Mirzaei (2010) developed a rational approach utilizing these strengths. The results of that rational approach were compared with more than 30 test specimens and found to be in a very good

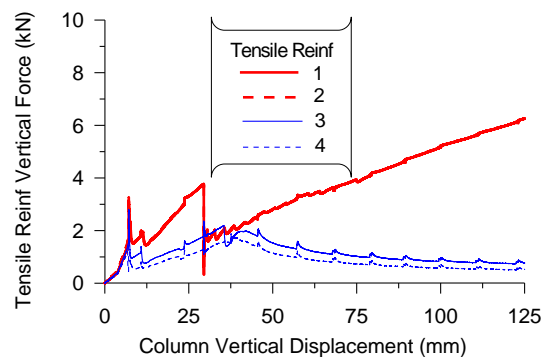


Fig. 10 Shear transferred through tensile reinforcement(see Fig. 3(b) for reinforcing bar locations)

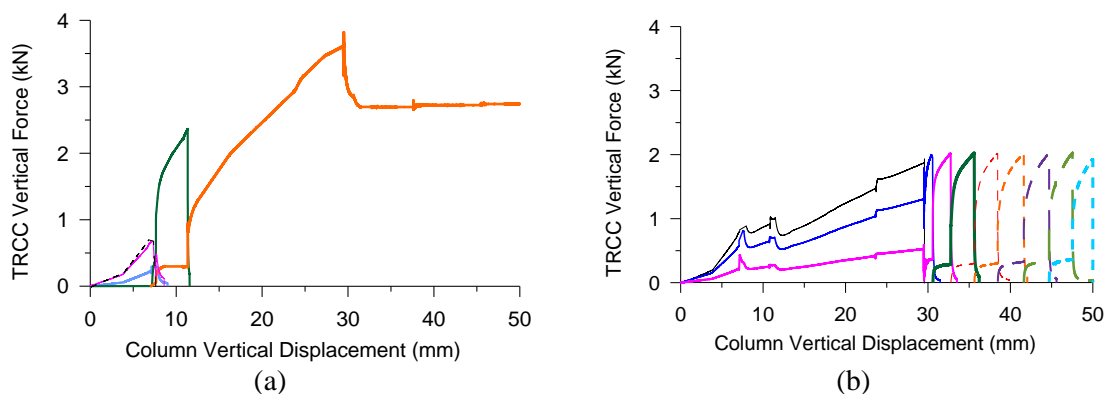


Fig. 11 Tensile Reinforcement-Concrete Connector (TRCC) forces for connectors (a) within punching cone and (b) within slab (outside punching cone) Connectors closest to punching cone boundary (Fig. 3(b)) fail sooner

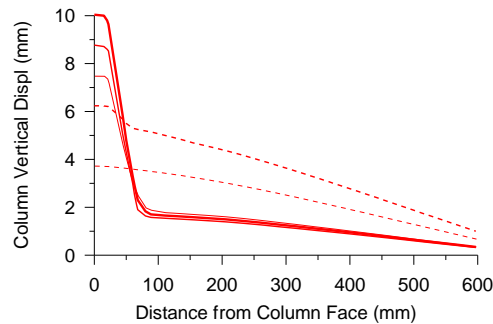


Fig. 12 Integrity bar deformed shapes before and after punching

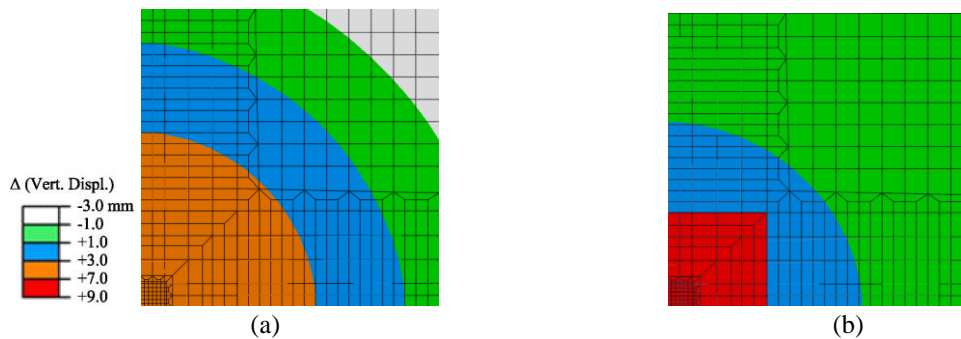


Fig. 13 Slab deflection contours (a) before and (b) after punching shear failure

agreement with the experimental data (Mirzaei 2010). Hence, only one test specimen, PM-11, has been chosen randomly here to compare its results with those of the numerical simulation method developed in this paper.

5. Progressive collapse resistance

Progressive collapse analysis of structures is carried out with different levels of model complexity (Weerheijm *et al.* 2009, Masoero *et al.* 2010, Valipour and Foster 2010, Yuan and Tan 2011). In this paper, in order to investigate the effects of the post-punching resistance in RC slabs after a column removal (explosion), a sixteen-column flat slab is designed according to ACI 318 (2011). Fig. 14 shows the geometry of the slab, which is assumed to be the structural system of an office building. The slab has 8 m and 6 m center-to-center spans in the x- and y-directions, respectively. The slab is 280 mm thick and the cross section of all columns is 300 × 300 mm.

The dimension of the slab is determined according to what frequently occurs in practice to be a good representative of actual structures. Müllers carried out an extensive study of 50 structures in Europe to determine the reasonable dimensions for flat slab analysis (Müllers 2007). The results of the study showed that the important geometrical properties (i.e., the span and slab thickness) of flat slab structures vary within a rather small range. The values used in this study are approximately the average of the ranges reported by Müllers (2007). Therefore, results obtained by the analyses of one slab structure have a general validity for these types of structures.

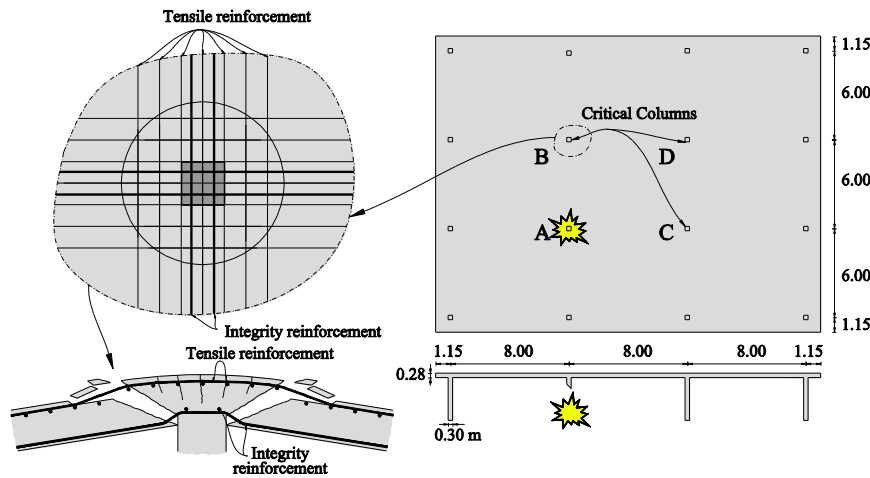


Fig. 14 Nonlinear dynamic FEM of system level study of progressive collapse due to punching shear failure

5.1 Slab gravity loads and design

Different load factors and load combinations are used for the design and progressive collapse evaluation according to the codes of practice (ACI 318 2011, GSA 2003). The following uniformly distributed loads for design of the slab are used. The slab self-weight is 7.0 kN/m^2 and other floor dead loads are set at 1.4 kN/m^2 . Assuming that one third of the floor is to be used as hallways and computer rooms the average design live load is set equal to 3.2 kN/m^2 . A live load reduction factor of 0.58 is used in design and finding the column axial load (ASCE-7 2010), therefore the reduced live load is $0.58 \times 3.2 = 1.85 \text{ kN/m}^2$. The ultimate floor load for design is about 13 kN/m^2 . The slab is designed against punching as it is the governing mode of failure at the ultimate limit state. The steel yield stress and concrete compressive strength are 500 MPa and 30 MPa, respectively. The slab punching strength is calculated according to ACI 318 (2011). The nominal punching strength is 965 kN (excluding the strength reduction factor of 0.75), which is comparable to the calculated punching strength based on the Critical Shear Crack Theory (Muttoni and Fernández 2008). The punching strength is 1067 kN based on Muttoni's refined model and is 980 kN based on this simplified method. The column axial force under the ultimate load combination is 722 kN which is almost equal to the punching strength of the slab ($0.75 \times 965 = 724 \text{ kN}$) leading to a satisfactory design of the structure. Based on the slab design, the flexural tensile reinforcement in the column strip at the interior column face consists of 20 mm diameter deformed bars at a spacing of 150 mm. In order to avoid reserved strength due to load combinations including lateral loads, it is assumed that the effects of lateral loads are small and the exterior (equivalent) frames are designed to resist lateral loads. For the progressive collapse analysis, the dead load is 8.4 kN/m^2 but the live load should be reduced according to GSA (2003), leading to a uniformly distributed progressive collapse analysis load of $1.0 \times 8.4 + 0.25 \times 3.2 = 9.2 \text{ kN/m}^2$. The column reaction under this load combination is 513 kN.

To design the integrity reinforcement, the design load is calculated using load factors of the accidental loading according to ACI 352.1R-89 (R2004). The amount of the integrity reinforcement is designed by

$$A_{si} = \frac{0.5q_d \ell_1 \ell_2}{\phi f_y} \quad (3)$$

where A_{si} is the minimum area of the integrity reinforcement in each principal direction placed over the column, q_d is the factored uniformly distributed load but not less than twice the slab service dead load, f_y is the yielding strength of steel, $\phi = 0.9$ is a shear reduction factor, and ℓ_1 and ℓ_2 are center-to-center span in each principal direction. The calculated integrity reinforcement consists of two 22 mm diameter deformed bars in each direction (see Fig. 14). The cross section area of the integrity reinforcement A_{si} may be multiplied by two thirds for edge connections, and by one-half for corner connections.

5.2 Modeling and simulation

The punching strength of the slab-column connection is calculated using Muttoni's refined model (Muttoni 2008). For the interior columns, the punching strength is 1067 kN. The elements (slab, punching cone, reinforcing bars, and nonlinear connectors) are defined in the FEM similar to those described in the static analysis (slab on single column). This model aims to demonstrate the vulnerability of flat slabs against punching shear failure after a column removal (explosion). The sudden removal of a column influences dynamically the rest of the slab and therefore the structure should be analyzed dynamically. First the structure is analyzed under the applied gravity loads and the forces at the top of column A are determined. Then, the column is removed from the model and instead, the column top forces from the previous step are applied to the slab, along with the gravity loads and the structure is analyzed again. The results (forces and displacements) of the two analyses are identical. Finally, forces in the opposite direction to the forces applied to the slab in place of the removed column are suddenly applied to the structure to simulate the column removal and dynamic analysis is conducted. The column is removed in two milliseconds because the results of a comprehensive experimental analysis showed that the failure time of a column can be chosen as close to zero (Sasani *et al.* 2007, Sasani and Sagiroglu 2008). A mass-proportional damping ratio of 0.05 in the first mode of vibration is used. The influence of the strain rate in the nonlinear FEM has been accounted for by Cowper-Symonds power law with a multiplier $D = 40$ and an exponent $n = 5$ (Abaqus Manual 2010). The simulation results show that the strain rate does not have a significant effect on the system responses.

5.3 Results and discussion

Fig. 15(a) shows the axial forces of neighboring columns B, C and D as a result of column A removal (explosion). The transferred shear force to column B increases and eventually exceeds the slab punching strength and drops significantly representing the occurrence of punching shear failure. The punching shear occurs at $t = 0.132$ sec. The axial forces in columns C and D increase considerably but do not lead to punching failure. The initial damage (column removal) led to the punching failure over column B, but could not propagate throughout the structure because no further punching is observed and the column forces stabilize at the end of the analysis, see Fig. 15(a). The column removal does not lead to the entire collapse of the structure because the structure is able to redistribute the loads and maintain its stability due in part to the post-punching Figs. 16(a) and (b) show the stress and strain histories of one of the integrity and tensile

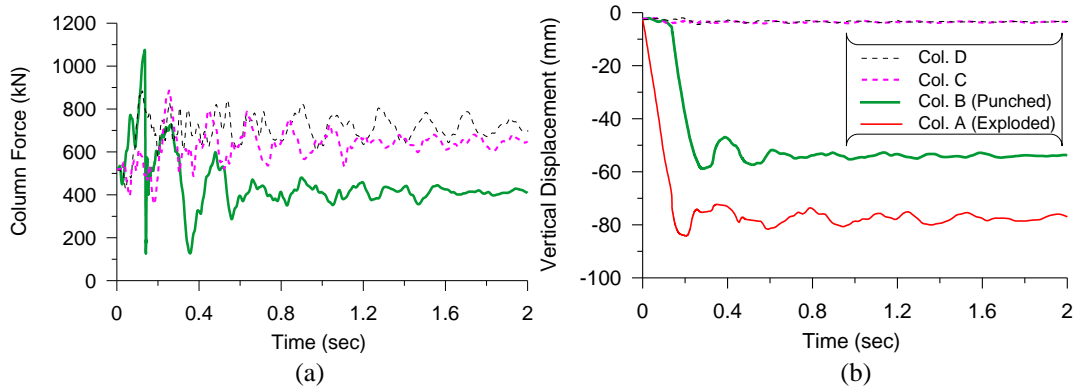


Fig. 15 (a) History of interior columns axial force and (b) history of slab displacement over interior columns after column removal

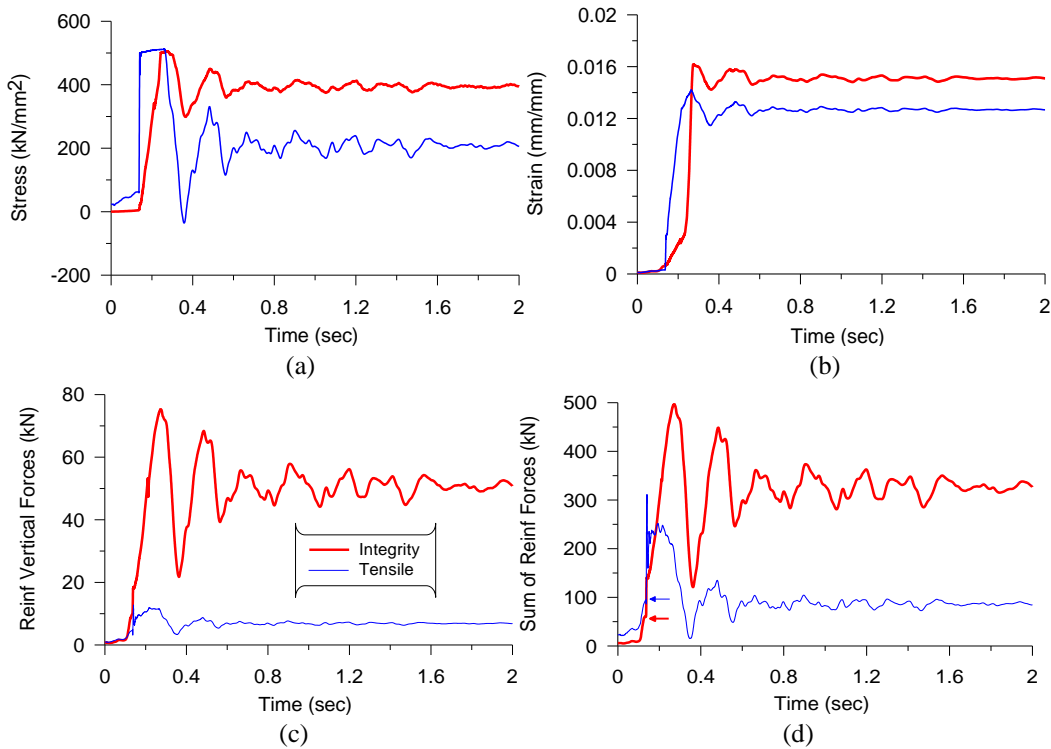


Fig. 16 (a) and (b) Stress and strain histories of integrity and tensile reinforcement in slab transversal direction over Column B, (c) shear transferred by one tensile and one integrity bar and (d) sum of shear transferred by all integrity and all tensile reinforcement

reinforcing bars in the slab transverse direction passing over Column B. The evolution of the shear transferred through the integrity bar as well as the tensile bar over the punched column is shown in Fig. 16(c). Both tensile and integrity reinforcement contribute to the shear transfer before punching. Before conducting the simulation, this contribution was assumed to be 15% of the punching strength. The simulation results show that right before punching, the sum of the contribution of

tensile and integrity reinforcement reached 16% of the punching load which is reasonable (65 kN from integrity and 94 kN from tensile reinforcement at $t = 0.132$ sec, as indicated by two arrows in Fig. 16(d)). Both contributions increase significantly as punching failure occurs because of the large relative vertical displacement occurring between the punching cone and the slab. As shown in Fig. 16(c), the transferred shear through the integrity reinforcing bar in the slab transverse direction reaches a peak of 75 kN and drops after punching and oscillates around 50 kN. The transferred shear through the central tensile reinforcement bar in the slab transversal direction reaches a peak of 13 kN and stabilizes at 7 kN in the post-punching phase. A significant difference can be seen in the amount of shear transferred by the integrity and tensile reinforcement after punching. It should be mentioned that all four integrity bars passing over the column remain active until the end of simulation but the number of involved tensile reinforcing bars decreases from fourteen before punching to six at the end of the simulation. The reason is that the tensile reinforcing bars that do not pass over the column and cross only the punching cone will lose their strength as the spalling of cover concrete on the slab side and the break-out of the punching cone continues. This can be an explanation as to why the sum of the contribution of all the tensile reinforcement in shear transfer decreases significantly from their peak strength (see Fig. 16(d)).

The punching shear failure occurs at a small deflection and consequently reinforcing bars passing through the punching cone become the only link between the slab and the punching cone.

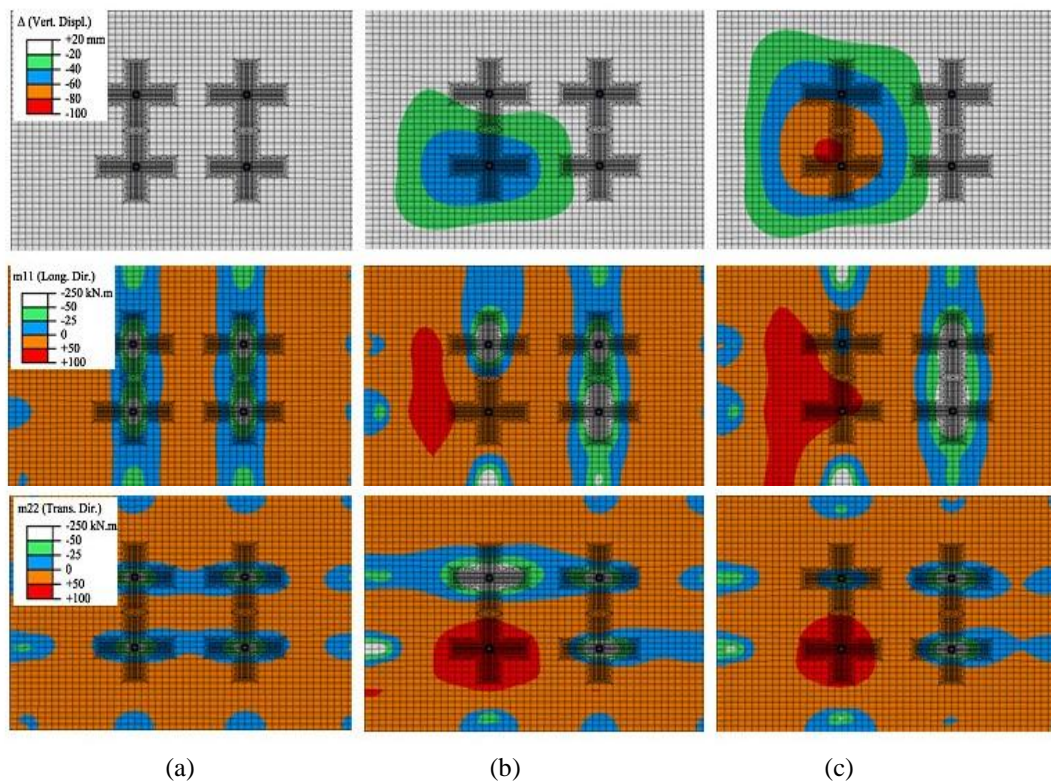


Fig. 17 Contours of slab vertical displacement and bending moments (m11 and m22) at (a) before column removal, (b) after column removal (right before punching), and (c) end of simulation

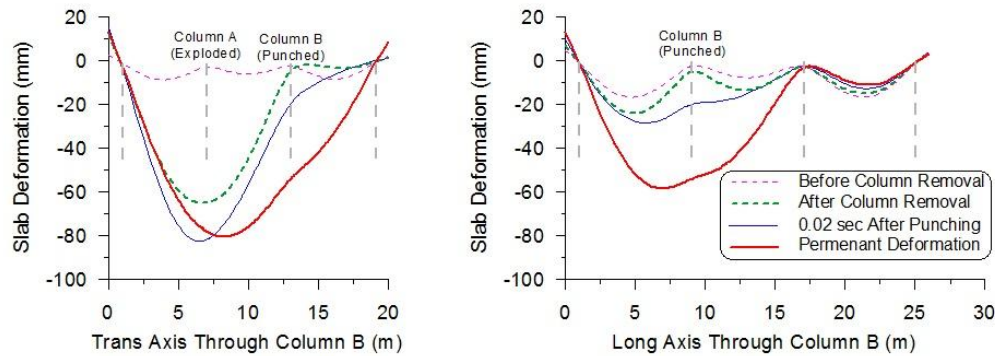


Fig. 18 Evolution of deformation of slab along transversal and longitudinal axes passing through punched column B

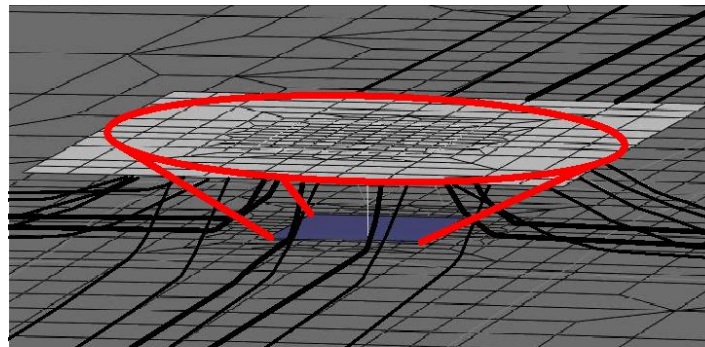


Fig. 19 Slab, punching cone, and reinforcing bars after punching failure (magnified)

The axial tensile forces developed in the slab reinforcing bars in the vicinity of the column increase for further deflection and in turn their vertical components contribute to the slab post-punching shear strength. In this simulation, the maximum vertical displacement of the slab with respect to the punching cone is about 58 mm. However, if the structure required deflecting more to redistribute the loads, the contribution of the integrity reinforcement in transferring load to the column could increase. This increase in the post-punching strength can help preventing the failure from propagating throughout the structure. The process of punching shear failure of a slab-column connection potentially leading to progressive collapse depends not only on the post-punching behavior of the connection but also on the overall behavior and structural characteristics of the region of the slab surrounding the damaged area and the punching strength of adjacent slab-column connections.

Fig. 17 shows the contours of slab deformation and slab bending moments in both principal directions (m_{11} and m_{22}) before column removal, after column removal (right before punching failure), and at the end of the simulation. The column removal in this flat slab structure triggers the punching failure to the adjacent column. In general, the failure can potentially propagate throughout the structure by consecutive punching failures leading to progressive collapse of a

large portion of the structure. The presence of the integrity reinforcement can provide an alternative load path for the load redistribution and prevent the structure from total collapse. In this study, it is assumed that the slab deformation away from the failure zone is negligible and consequently a linear behavior is considered. A comparison of the bending moments obtained from FEM can be of interest to verify this assumption. The negative yield moment capacity of the slab ($M_c = 233$ kN.m/m) is compared with the maximum bending moments in both directions. As Fig. 17 shows, the slab bending moment is less than M_c almost everywhere except for a few small elements in the vicinity of the columns (with a maximum moment of 247 kN.m/m). Furthermore, positive bending moments obtained by FEM are always less than the positive moment capacity of the slab. Therefore, the assumption of linear slab elements for flexure is reasonably verified.

Fig. 18 displays the evolution of the deformation of the slab along both (transverse and longitudinal) axes passing through the punched column B. The slab deformation before and after the punching shear failure, and at the end of the simulation is shown. And finally, Fig. 19 shows the slab, punching cone and the reinforcing bars in the vicinity of the punched column after punching failure. The boundary of the actual punching cone shape is also shown. It clearly shows that the slab suspends from the punching cone by means of the integrity and tensile reinforcement. This configuration is quite similar to what happens in failure due to punching shear.

5.4 Influence of slab geometry, material properties and reinforcement layout

The effects of various parameters defining the slab-column connections on the punching and post-punching behavior were previously studied for the rational approach and the results of the parametric study were in agreement with that of experimental results (Mirzaei 2010). These parameters include reinforcement ratio, slab thickness, column width, angle of inclination of punching cone, yield strength and ultimate strain of tensile/integrity reinforcement, concrete compressive strength, and concrete cover. The influence of each parameter on the punching strength was studied, as well as each parameter's effect on the contribution of tensile and integrity reinforcement to the post-punching strength of the slab.

It was generally concluded that for

- Punching strength: the increase of slab thickness, concrete compressive strength and column width increases the punching strength and the effects of other parameters are negligible.
- Tensile reinforcement contribution: the increase of slab thickness, concrete compressive strength and concrete cover increases the contribution of tensile reinforcement to post-punching resistance and the effects of other parameters are negligible.
- Integrity reinforcement contribution: the increase of slab thickness, ultimate strain and yield strength and diameter of steel reinforcement increases the contribution of integrity reinforcement to post-punching resistance and the effects of other parameters are negligible.
- Based on these conclusions and the fact the breakout and spalling strength of the rational model (Mirzaei 2010) are used in the numerical simulation in this paper, one can further conclude that for the sixteen-column flat slab:
 - Slab thickness: the increase of slab thickness increases both punching and post-punching strength. However, a thicker slab means higher demand and to resist progressive collapse in the event of extreme loading conditions, we still need to provide the required integrity reinforcement.
 - Column dimensions: the increase of column dimensions increases the punching strength but has practically no influence on the post-punching strength. The bigger column means higher demand on the system which in case of an accident needs to be redistributed throughout the

structure and if enough post-punching resistance is not provided will lead to a progressive collapse of the system.

Other parameters such as the yield strength and ultimate strain of tensile/integrity reinforcement, concrete compressive strength, and concrete cover which increase the post-punching strength but do not necessarily increase structural demand will help the structure to resist progressive collapse in the event of abnormal loading conditions.

6. Conclusions

The failure of RC slabs is in most cases ductile and causes limited load redistribution. Punching failure of flat slabs without shear reinforcement, however, is brittle and occurs with small deflection and almost no warning signs. The drop in resistance at punching failure is considerable and leads to a large redistribution of loads, which can trigger failure at adjacent columns and eventually the collapse of entire or large parts of the structure. An analytical model to reliably evaluate the progressive collapse resistance of a flat slab structure and redistribution of gravity loads through alternative load paths is required to account for the slab post-punching resistance and in turn for the discontinuity developed due to punching. Such an analytical model is proposed in this paper. The modeling technique is used to study response of a slab on a single column as well as progressive collapse resistance of a flat slab structure. The key components of the model, which allow the slab-punching cone discontinuity after punching, include:

- 1)The Slab-Column Shear Connectors (SCSC), which attach the slab to the column and fail when the punching strength of the slab is reached.

- 2)The punching cone, which supports the slab through the slab reinforcement after punching.

- 3)Tensile and integrity reinforcing bars, which are explicitly modeled and connected to the slab and punching cone.

- 4)Reinforcement-Concrete Connectors (RCC), which attach the tensile and integrity reinforcement to the slab and punching cone, as applicable. These connectors simulate concrete breakout and spalling.

The modeling technique is validated using experimental results. It is shown that simulation results obtained from the model are in good agreement with experimental data.

The dowel action is modeled explicitly. Depending on the slab geometry and concrete and steel mechanical characteristics, the contribution of dowel action to punching strength is reported to be up to about 30% (Kinnunen *and* Nylander 1960, Hewitt and Batchelor 1975, Long 1975, Fib 2011, Muttoni *and* Fernández 2008). In the case of slab on a single column, 24% of the punching strength is found in this study to be due to the dowel action. This contribution in the case of the flat slab structure is about 16%.

In addition to the dowel action, the effect of longitudinal reinforcement on flexural resistance and in turn on punching shear is discussed. It is argued that while a decrease in the amount of longitudinal reinforcement of a slab will lead to a smaller load at which punching occurs, this is primarily due to the flexural rebar yielding and limiting the amount of force that can be transferred to the column. In other words, the slab reduced flexural strength does not allow a larger shear force demand developed as opposed to the shear resistance being reduced.

In order to evaluate the effects of punching shear in progressive collapse analysis of structural systems, the response of a flat slab structure following loss (explosion) of a column is studied. It is demonstrated that in spite of the complexity of numerical simulation following the formation of a

significant discontinuity, post-punching response can be effectively modeled at a system level. Under the load combination according to GSA (2003), the interior column axial force is 513 kN. Simulation results show that following removal (explosion) of column A, the neighboring column B will be overloaded and experience punching shear. The punching strength of the column is 1067 kN. The axial forces in columns C and D increase considerably but do not lead to punching failure. This is due in part to the fact that the slab at the top of punched column B could transfer about 400 kN force at the end of simulation. Therefore, it is demonstrated that post-punching resistance of a slab helps prevent progressive collapse of reinforced concrete structures following an explosion.

The slab post-punching shear strength is primarily provided by the integrity reinforcement. That is, the contribution of tensile reinforcement is less than one quarter of the slab post-punching strength at the end of the simulation (final equilibrium stage). This is due to the fact that the four integrity bars passing through the column remain active until the end of simulation but the number of contributing tensile reinforcing bars decreases from fourteen before punching to six at the end of the simulation. The reason is that the tensile reinforcement bars that do not pass over the column top and cross only the punching cone will lose their strength as the spalling of cover concrete and the break-out of the punching cone continues. The simulation results also show that the strain rate does not have a significant effect on the system responses.

Acknowledgements

This material is based upon work supported by the U.S. Department of Homeland Security under Award Number 2008-ST-061-ED0001. The views and conclusions contained in this document are those of the authors and should not be interpreted as necessarily representing the official policies, either expressed or implied, of the U.S. Department of Homeland Security.

References

- Abaqus INC (2010), *Standard User's Manual*, 6.9 Edition.
- ACI 318 (2011), *Building Code Requirements for Structural Concrete*, ACI 318-11, American Concrete Institute, Committee 318, USA.
- ACI 349 (2001), *Code Requirements for Nuclear Safety Related Concrete Structures*, ACI 349-01, American Concrete Institute, USA.
- ACI 352.1R-11 (2011), *Guide for Design of Slab-Column Connections in Monolithic Concrete Structures*, ACI Committee 352, American Concrete Institute, USA.
- Joint ACI-ASCE Committee 426 (1974), *Shear strength of reinforced concrete members-slabs*, *Proceedings of ASCE*, **100** (ST8).
- ASCE 7 (2010), *Minimum Design Loads for Buildings and Other Structures*, ASCE, SEI/ASCE-7, USA
- Bao, Y., Kunnath, S.K., El-Tawil, S.H. and Lew, H.S. (2008), "Macromodel-based simulation of progressive collapse: RC frame structures", *J. Struct. Eng.*, **134**(7), 1079-1091.
- Carino, N.J., Woodward, K.A., Leyendecker, E.V. and Fattal S.G. (1983), "A review of the Skyline Plaza collapse", *Concr. Int.*, **5**(7), 35-42.
- Corley, W.G. (2004), "Lesson learned on improving resistance of buildings to terrorist attacks", *J. Perform. Construct. Facil.*, *ASCE*, **18**(2), 68-78.
- DOD (2010), *Unified Facilities Criteria, Design of Buildings to Resist Progressive Collapse*, US Department of Defense, Washington DC, USA.
- Ellingwood, B., Smilowitz, R., Dusenberry, D., Duthinh, D. and Carino, J.N. (2007), *BestPractices for*

- Reducing the Potential for Progressive Collapse in Buildings, National Institute of Standards and Technology, Technology Administration, U.S. Department of Commerce, USA.
- Fib (2001), *Punching of Structural Concrete Slabs*, fib bulletin 12, Fédération Internationale du Béton, Lausanne, Switzerland.
- GSA (2003), *Progressive Collapse Analysis and Design Guidelines for New Federal Office Buildings and Major Modernization Projects*, General Services Administration, USA.
- Guandalini, S. (2005), *Poinçonnement Symétrique des Dalles en Béton Armé*, Thèse de doctorat, N. 3380, Lausanne, Switzerland.
- Guandalini, S., Burdet, O. and Muttoni, A. (2009), "Punching tests of slabs with low reinforcement ratios", *ACI Struct. J.*, **106**(1), 87-95.
- Hewitt, B.E. and Batchelor, B. (1975), "A punching shear strength of restrained slabs", *J. Struct. Div., ASCE*, **101**(9), 1837-1853.
- Jelic, I., Pavlovic, M.N., Kotsovos, M.D. (1999), "A study of dowel action in reinforced concrete beams", *Mag. Concr. Res.*, **2**(2), 131-141.
- Kaminetzky, D. (1991), *Design and Construction Failures Lessons from Forensic Investigations*, McGraw-Hill, USA.
- King, S. and Delatte, N.J. (2004), "Collapse of 2000 commonwealth avenue: punching shear case study", *Perform. Construct. Facil. ASCE*, **18**(1), 54-61.
- Kinnunen, S. and Nylander, H. (1960), *Punching of Concrete Slabs Without Shear Reinforcement*, *Transactions of the Royal Institute of Technology*, No. 158, Stockholm, Sweden.
- Knoll, F. and Vogel, T. (2009), *Design for Robustness*, Structural Engineering Documents 11, IABSE-AIPC-IVBH, Switzerland.
- Long, A.E. (1975), "A two-phase approach to the prediction of the punching strength of slabs", *ACI Struct. J.*, **72**(2), 37-45.
- Masoero, E., Wittel, F.K., Herrmann, H.J. and Chiaia, B.M. (2010), "Progressive collapse mechanisms of brittle and ductile framed structures", *J. Eng. Mech., ASCE*, **136**(8), 987-995.
- Melo, G.S. and Regan, P.E. (1998), "Post-punching resistance of connections between flat slabs and interior columns", *Mag. Conc. Res.*, **50**(4), 319-327.
- Mirzaei, Y. (2010), *Post-Punching Behavior of Reinforced Concrete Slabs*, EPFL Thesis No. 4613, Lausanne, Switzerland.
- Müllers, I. (2007), "Zur Robustheit im Hochbau: Stützensausfall als Gefährdungsbild für Stahlbetontragwerke", Ph.D. Thesis, ETH, Zurich, Switzerland.
- Mirzaei, Y. and Muttoni, A. (2008), *Tests of the Post-Punching Behavior of the Reinforced Concrete Flat Slabs*, IS-BETON, Lausanne, Switzerland.
- Mitchell, D. and Cook, W.D. (1984), "Preventing progressive collapse of slab structures", *J. Struct. Eng., ASCE*, **110**(7), 1513-1532.
- Muttoni, A. (2008), "Punching shear strength of reinforced concrete slabs without transverse reinforcement", *ACI Struct. J.*, **105**(4), 440-450.
- Muttoni, A. and Fernández, R.M. (2008), "Shear strength of members without transverse reinforcement as function of critical shear crack width", *ACI Struct. J.*, **105**(2), 163-172.
- Park, R. (1964), "Tensile membrane behavior of uniformly loaded rectangular reinforced concrete slabs with fully restrained edges", *Mag. Conc. Res.*, **16**(40), 39-44.
- Sasani, M., Bazan, M. and Sagioglu, S. (2007), "Experimental and analytical progressive collapse evaluation of actual reinforced concrete structure", *ACI Struct. J.*, **104**(6), 731-739.
- Sasani, M. and Sagioglu, S. (2008), "Progressive collapse of reinforced concrete structures: a multihazard perspective", *ACI Struct. J.*, **105**(1), 96-103.
- Schousboe, I. (1976), "Bailey's crossroads collapse reviewed", *J. Construct. Div., ASCE*, **102**(CO2), 365-378.
- Sozen, M.A., Corley, W.G., Mlakar, P.F. and Thornton, C.H. (1998), "The Oklahoma city bombing: structural details and possible mechanisms for the Murrah building", *J. Perform. Construct. Facil.*, **12**(3), 120-136.

- Theodorakopoulou, D.D. and Swamy, R.N. (2002), "Ultimate punching shear strength analysis of slab-column connections", *Cement Concrete Compos.*, Special Theme Issue, **24**(6), 509-521.
- Valipour, H.R. and Foster, S.J. (2010), "Nonlinear analysis of 3D reinforced concrete frames: effect of section torsion on global response", *Struct. Eng. Mech.*, **36**(4), 421-445.
- Weerheijm, J., Mediavilla, J. and Van Doormaal, J.C.A.M. (2009), "Explosive loading of multi-story RC buildings: Dynamic response and progressive collapse", *Struct. Eng. Mech.*, **32**(2), 193-212.
- Yuan W.F. and Tan K.H. (2011), "Modeling of progressive collapse of a multi-story structure using a spring-mass-damper system", *Struct. Eng. Mech.*, **37**(1), 79-93.

CC